

Multiple Switching Patterns for SHEPWM Inverters Using Differential Evolution Algorithms

Ayong Hiendro

Department of Electrical Engineering, Tanjungpura University
JalanJend. A. Yani, Pontianak 78124, Indonesia
e-mail: ayongh2000@ieee.org

Abstract

An investigation on multiple patterns for both odd and even number of switching angles in a three-phase selective harmonic elimination pulse width modulation (SHEPWM) inverter is presented. The switching patterns are examined and classified on the basis of the harmonic performance of the waveforms output from the inverter. Differential evolution algorithms are employed to calculate the optimum switching angles. Selected cases are verified experimentally by a digital signal processor-based hardware implementation. The experimental results show that all types of the patterns offer low harmonic distortions on the inverter output after filtering. However, one type gives better harmonic performance is identified.

Keywords: differential evolution algorithms, multiple solution, pulse width modulation, selective harmonic elimination

1. Introduction

Selective harmonic elimination pulse width modulation (SHEPWM) has been widely studied as an alternative to traditional PWM techniques. SHEPWM can be use to eliminate specific undesired lower-order harmonic components from output of single- or three-phase inverters and to control its fundamental. The remaining higher-order harmonics are then suppressed by using a small L-C passive filter.

Many computational methods have been proposed in [1]-[15] to determine optimum switching angles in order to eliminate the specific lower-order harmonics. Single set of solution for the SHEPWM within 60° or 90° has been presented in [1]-[7]. Another set of solution for the switching angles is also reported in [8]-[10].

Multiple sets of solutions for the SHEPWM problem have been a concern in [11]-[15]. Kato [11] finds all possible multiple switching patterns for the SHEPWM problems by employing sequential homotopy-based computation. In the paper [11], he also shows eight different solution patterns for 9 switching angles case in a three-phase inverter for all values of modulation indices ($0 \leq |M| \leq 1.15$). Agelidis et al. use a minimization technique to investigate multiple switching patterns for the SHEPWM bipolar [12], [13] and unipolar [14] waveforms and identify better set of solutions with respect to harmonic distortion factor (HDF) and amplitude of the most significant harmonics. They also present multiple solution patterns for 3, 5 and 7 switching angles cases in a three-phase inverter [12], and in both single- and three-phase inverters [13]. Jabr [15] presents the same vein work reported in [9]-[12] but he uses a different computational method to find all solutions of the SHEPWM problems. However, the multiple solution patterns for even N are not shown in [10]-[14]. So far, there are only several multiple solution patterns for certain odd number of switching angles that have been reported in [11]-[15] and there has been no comprehensive assessment of all patterns available in both odd and even number of switching angles.

The objective of this paper is to report multiple of solutions available for both odd and even number of switching angles problems in a two level SHEPWM inverter for three-phase applications. The solution patterns for the positive value of modulation index (M) in the range of the SHEPWM capability ($0 \leq M \leq 1.15$) [16] are investigated. The patterns of each number of angles are identified and classified with respect to their general pattern forms. Performance of each type of pattern is evaluated and compared on the basis of total harmonic distortion (THD) of the inverter output waveform. In this paper, differential evolution algorithms (DE) [17] are applied to calculate the optimum switching angles of the SHEPWM problems. Finally, experimental results are presented to validate the theoretical arguments.

2. Schemes for Selective Harmonic Elimination in Three-Phase Inverters

There are two possible schemes for two-level switching on a three-phase inverter configuration depending on the number of switching angles. Each scheme has its specific PWM switching function.

2.1. Two-Level Switching Scheme for Odd Value of Angles

The PWM pattern with odd value of switching angles is shown in Fig.1. The angle is rising notch transition at the beginning of the cycle. As the pattern is odd quarter-wave symmetry, only odd-order harmonic components exist. The Fourier series expansion of this output voltage waveform is written as

$$v(\omega t) = \sum_{n=1,5,7,\dots}^{\infty} V_n \sin(n\omega t) \quad (1)$$

For no triplen-order harmonics exist, the magnitude of harmonic components (including the fundamental) V_n is defined by

$$V_n = \frac{4V_{dc}}{n\pi} \left[-1 - 2 \sum_{k=1}^N (-1)^k \cos(n\alpha_k) \right] \quad (2)$$

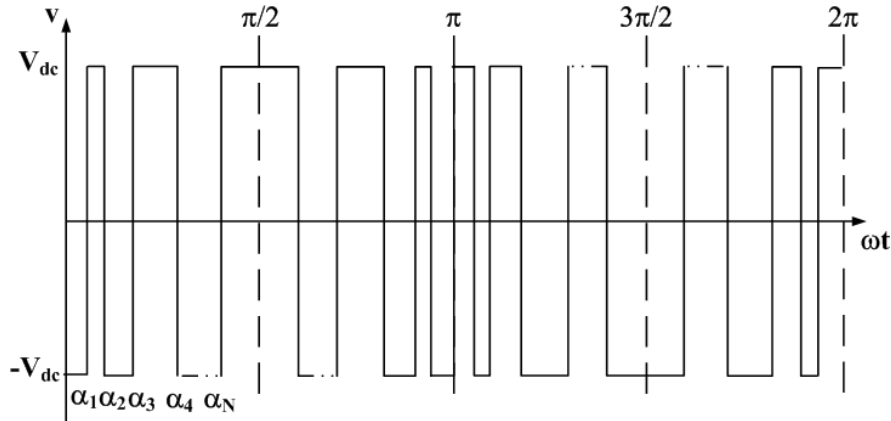


Figure 1. Two-level PWM waveform for odd value of angles

Harmonic elimination concerns to eliminate $(N-1)$ harmonics completely from the waveform through calculating of N switching angles in the first quarter period. The remaining one equation is reserved for controlling the fundamental magnitude V_1 at a particular modulation index value. Hence, the equations for solving the N switching angles $\alpha_1, \alpha_2, \dots, \alpha_N$ are arranged into

$$\begin{aligned} f_1(\alpha) &= \frac{4}{\pi M} \left[-1 - 2 \sum_{k=1}^N (-1)^k \cos(\alpha_k) \right] - 1 \\ f_5(\alpha) &= \frac{4}{5\pi M} \left[-1 - 2 \sum_{k=1}^N (-1)^k \cos(5\alpha_k) \right] \\ f_7(\alpha) &= \frac{4}{7\pi M} \left[-1 - 2 \sum_{k=1}^N (-1)^k \cos(7\alpha_k) \right] \\ &\vdots \\ f_{(3N-2)}(\alpha) &= \frac{4}{(3N-2)\pi M} \left[-1 - 2 \sum_{k=1}^N (-1)^k \cos((3N-2)\alpha_k) \right] \end{aligned} \quad (3)$$

where $f_5, f_7, \dots, f_{(3N-2)}$ are the normalized magnitude (with respect to the fundamental) of harmonics to be eliminated and $M = V_1/V_{dc}$ is the modulation index.

The objective function created for optimization is expressed by

$$\begin{aligned} f(\alpha) &= |f_1| + |f_5| + |f_7| + |f_{11}| + |f_{13}| + \dots + |f_{(3N-1)}|, \\ &|f_1|, |f_5|, |f_7|, |f_{11}|, |f_{13}|, \dots, |f_{(3N-1)}|, f < \varepsilon \end{aligned} \quad (4)$$

and the solutions must satisfy the conditions

$$\alpha_1 < \alpha_2 < \dots < \alpha_N < 90^\circ \quad (5)$$

with the desired level of accuracy ε .

Once the switching angles $\alpha_1, \alpha_2, \dots, \alpha_N$ are found, the rest of angles are calculated by

$$\begin{aligned} \alpha_k &= 180^\circ - \alpha_{(2N+1)-k}, \text{ for } k = N+1 \text{ to } 2N, \\ \alpha_{2N+1} &= 180^\circ, \\ \alpha_k &= 360^\circ - \alpha_{(4N+2)-k}, \text{ for } k = 2N+2 \text{ to } 4N+1, \\ \alpha_{4N+2} &= 360^\circ \end{aligned} \quad (6)$$

Each pulse width (PW) between two consecutive switching angles for the cycle duration T (as shown in Fig. 1) is specified by

$$PW_k = (\alpha_{2k} - \alpha_{2k-1})T/360^\circ, \text{ for } k = 1 \text{ to } 2N+1 \quad (7)$$

2.1. Two-Level Switching Scheme for Even Value of Angles

The PWM pattern with even value of switching angles is shown in Fig.2, in which the switching angle is falling notch transition at the beginning of the cycle. The Fourier series of the waveform is similar to (1), but V_n is defined as follows:

$$V_n = \frac{4V_{dc}}{n\pi} \left[1 + 2 \sum_{k=1}^N (-1)^k \cos(n\alpha_k) \right] \quad (8)$$

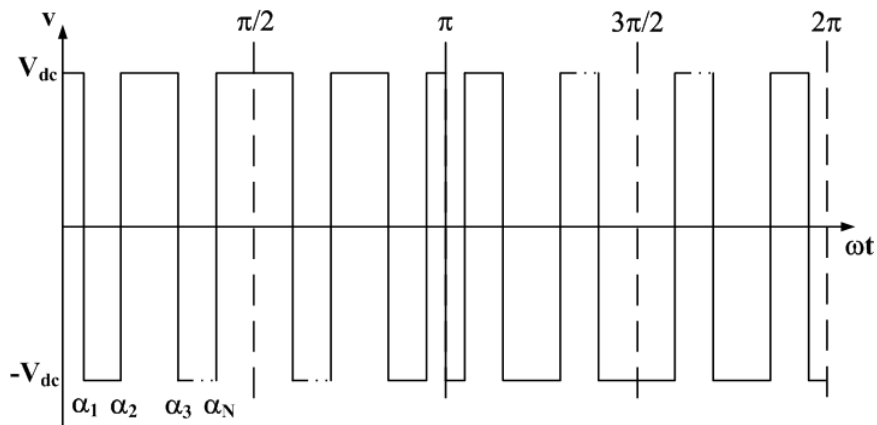


Figure 2. Two-level PWM waveform for even value of angles

The equations for solving the N switching angles $\alpha_1, \alpha_2, \dots, \alpha_N$ are arranged into

$$\begin{aligned} f_1(\alpha) &= \frac{4}{\pi M} \left[1 + 2 \sum_{k=1}^N (-1)^k \cos(\alpha_k) \right] - 1 \\ f_5(\alpha) &= \frac{4}{5\pi M} \left[1 + 2 \sum_{k=1}^N (-1)^k \cos(5\alpha_k) \right] \\ f_7(\alpha) &= \frac{4}{7\pi M} \left[1 + 2 \sum_{k=1}^N (-1)^k \cos(7\alpha_k) \right] \\ &\vdots \\ f_{(3N-1)}(\alpha) &= \frac{4}{(3N-1)\pi M} \left[1 + 2 \sum_{k=1}^N (-1)^k \cos((3N-1)\alpha_k) \right] \end{aligned} \quad (9)$$

where $f_5, f_7, \dots, f_{(3N-1)}$ are the normalized magnitude of the harmonics to be eliminated. The objective function for optimization is similar to (4) and must satisfy the same conditions as in (5).

As shown in Fig. 2, the waveform is started by $\alpha_0 = 0^\circ$ and once the switching angles $\alpha_1, \alpha_2, \dots, \alpha_N$ are found, the rest of the angles can be calculated by

$$\begin{aligned}
\alpha_k &= 180^\circ - \alpha_{(2N+1)-k}, \text{ for } k = N+1 \text{ to } 2N, \\
\alpha_{2N+1} &= 180^\circ, \\
\alpha_k &= 360^\circ - \alpha_{(4N+2)-k}, \text{ for } k = 2N+2 \text{ to } 4N+1
\end{aligned} \tag{10}$$

The pulse width (PW) between two consecutive switching angles as shown in Fig. 2 can be expressed as follows:

$$PW_k = (\alpha_{2k-1} - \alpha_{2k-2})T/360^\circ, \text{ for } k = 1 \text{ to } 2N+1 \tag{11}$$

3. Differential Evolution Algorithms for Optimization of Switching Angles

The main procedures in DE are initialization, mutation, crossover or recombination and selection. The initial population is randomly selected and should cover the entire parameter space. The mutant individuals are created by adding the weighted difference between two parent individuals. Then, the parameter of the mutant individual and the parent individual are mixed to yield the trial individual. If the trial individual is better than the parent individual, then the trial individual replaces the parent individual in the next generation.

The following is the working algorithms involved in employing the DE to determine optimized switching angles:

1) *Parameters setup.* The parameters to be set for the DE to work consist of objective parameter (N), population size (NP), mutation factor (F), crossover rate (CR) and boundaries. In this application, the objective parameter specifies the number of optimized switching angles. The boundaries must satisfy (5) and both F and CR are in the range of $[0, 1]$.

2) *Initialization of the population.* The first step in the DE optimization process is to create an initial population of switching angles as the candidate solutions by assigning random values to each boundary. Such switching angle must lie inside the feasible bounds (lower and upper bounds). The initialization is assigned by

$$\begin{aligned}
\alpha_{i,j}^{(0)} &= \alpha_{minj} + rand_j(\alpha_{maxj} - \alpha_{minj}), \\
i &= 1, 2, \dots, NP, \quad j = 1, 2, \dots, N
\end{aligned} \tag{12}$$

where $\alpha_{i,j}^{(0)}$ is the initial population (generation $G = 0$) of candidate solutions, α_{minj} and α_{maxj} are the lower and upper bounds of j^{th} decision switching angles, and $rand_j$ is a random value within $[0,1]$ generated according to a uniform probability distribution.

3) *Evaluation of the initial population.* Evaluating the fitness value of each switching angle of the population is carried out by using (4). The best switching angle $\alpha_{bestj}^{(0)}$ and the best value $f_{best}^{(0)}$ are then selected by using

$$f_{best}^{(0)} = f(\alpha_{bestj}^{(0)}), \quad \alpha_{bestj}^{(0)} \in \alpha_{i,j}^{(0)} \tag{13}$$

4) *Mutation operation (differential operation).* Mutation or differential operator creates a mutant switching angle by perturbing a randomly selected switching angle with the difference of the two other randomly selected switching angles. All of these switching angles must be different from each other. To control the perturbation and improve convergence, the difference between two switching angles is amplified by a mutation factor F , a constant in the range of $[0, 1]$. For each parent (target) switching angle $\alpha_{i,j}^{(G)}$, a mutant switching angle $v_{i,j}^{(G)}$ is produced using one of the following mutation variants:

$$DE/rand/1: \quad v_{i,j}^{(G+1)} = \alpha_{ra,j}^{(G)} + F(\alpha_{rb,j}^{(G)} - \alpha_{rc,j}^{(G)}) \tag{14}$$

$$DE/best/1: \quad v_{i,j}^{(G+1)} = \alpha_{bestj}^{(G)} + F(\alpha_{ra,j}^{(G)} - \alpha_{rb,j}^{(G)}) \tag{15}$$

$$DE/rand-to-best/1: \quad v_{i,j}^{(G+1)} = \alpha_{i,j}^{(G)} + F(\alpha_{bestj}^{(G)} - \alpha_{i,j}^{(G)}) + F(\alpha_{ra,j}^{(G)} - \alpha_{rb,j}^{(G)}) \tag{16}$$

$$DE/best/2: \quad v_{i,j}^{(G+1)} = \alpha_{bestj}^{(G)} + F(\alpha_{ra,j}^{(G)} - \alpha_{rb,j}^{(G)}) + F(\alpha_{rc,j}^{(G)} - \alpha_{rd,j}^{(G)}) \tag{17}$$

$$DE/rand/2: \quad v_{i,j}^{(G+1)} = \alpha_{ra,j}^{(G)} + F(\alpha_{rb,j}^{(G)} - \alpha_{rc,j}^{(G)}) + F(\alpha_{rd,j}^{(G)} - \alpha_{re,j}^{(G)}) \tag{18}$$

where the indices $ra, rb, rc, rd, re \in \{1, 2, \dots, NP\}$ are randomly chosen mutually exclusive integers and must be different from each other and all are different from the base index i . The angles $\alpha_{ra,j}^{(G)}$, $\alpha_{rb,j}^{(G)}$ and $\alpha_{rc,j}^{(G)}$ are the shuffled individuals from the population $\alpha_{i,j}^{(G)}$, while $G = 0, 1, 2, \dots, G_{max}$ denotes the subsequent generation created for each iteration (generation). The angle $\alpha_{bestj}^{(G)}$ is the best switching angle with the best fitness in the population at generation G .

5) *Crossover operation (recombination)*. Following the mutation operation, crossover is applied to the population. Crossover operator is used to increase the diversity of the mutant switching angles. It generates a trial switching angle $t_{i,j}^{(G+1)}$. The trial switching angle is a combination of $v_{i,j}^{(G+1)}$ and $\alpha_{i,j}^{(G)}$ based either on binomial scheme (*bin*) or on exponential scheme (*exp*). In the binomial scheme, if the random number is less or equal than CR , the parameter will come from $v_{i,j}^{(G+1)}$, otherwise the parameter comes from $\alpha_{i,j}^{(G)}$. If $CR = 1$, it means that $t_{i,j}^{(G+1)}$ will be composed entirely of $v_{i,j}^{(G+1)}$. The binomial crossover can be expressed as

$$t_{i,j}^{(G+1)} = \begin{cases} v_{i,j}^{(G+1)} & \text{if } (rand_j \leq CR) \text{ or } (j = j_{rand}) \\ \alpha_{i,j}^{(G)} & \text{otherwise} \end{cases} \quad (19)$$

where $i = 1, 2, \dots, NP$, $j = 1, 2, \dots, N$, and j_{rand} is a randomly chosen index $\in \{1, 2, \dots, N\}$ that guarantees $t_{i,j}^{(G+1)}$ to get at least one parameter from $v_{i,j}^{(G+1)}$.

6) *Selection operation*. Finally, $t_{i,j}^{(G+1)}$ yielded from the crossover operation is accepted for the next generation if and only if it has an equal or lower value of the objective function than that of its parent $\alpha_{i,j}^{(G)}$. It can be expressed as follows:

$$\alpha_{i,j}^{(G+1)} = \begin{cases} t_{i,j}^{(G+1)} & \text{if } f(\alpha_{i,j}^{(G+1)}) \leq f(\alpha_{i,j}^{(G)}) \\ \alpha_{i,j}^{(G)} & \text{otherwise} \end{cases} \quad (20)$$

The best switching angle and value of the current generation are also selected in here as

$$f_{best}^{(G+1)} = f(\alpha_{bestj}^{(G+1)}), \quad \alpha_{bestj}^{(G+1)} \in \alpha_{i,j}^{(G+1)} \quad (21)$$

The mutation, crossover and selection processes are repeated to create a new next generation until $f_{best}^{(G+1)}$ meets its criterion ε and results in $\alpha_{bestj}^{(G+1)}$ as the satisfied switching angle.

4. Research Method

Preparation of objective functions. Sets of objective function for both odd and even value of angles are prepared for satisfying DE algorithms. Objective functions for solving N switching angles are equation (3) for odd value of angles and equation (9) for even value of angles, respectively.

Employing DE algorithms. In this application, objective parameter (N) specifies the number of optimized switching angles and then population size of $10N$ is selected. For instant if $N = 7$, $NP = 70$ is employed. Determining F and CR should be used is quite difficult and in this work a repetitive looping command is inserted into the DE algorithms to search the best combinations of F and CR . There are five commonly used variants in DE as expressed by equations (14) – (18). All variants are used to find the optimized switching angles. The variant which needs the less iteration is then used in the DE optimization. The algorithms are implemented by setting up $\varepsilon = 0.0001$ to find all sets of solution. Every sets of switching angles are founded for the modulation indices set from 0.0 to 1.15.

Experimental verification. To verify performances of the switching patterns, the inverter was implemented with TMS320C17 digital signal processor. The experiments were carried out with the following parameters: $V_{dc} = 50V$, $L = 10mH$, $C = 12\mu F$, $R = 20\Omega$, and $f = 50Hz$.

5. Results and Analysis

Figures 3-6 illustrate various series of the switching patterns for both odd and even values of the switching angles. The types of patterns can be classified with respect to their orderliness pattern forms. Each type possesses the same basic characteristics and resemblances. Every notch of switching patterns is founded for all over positive values of M in the range $0 \leq M \leq 0.15$. However, some patterns exceed 90 degrees (i.e. $N = 2$, type-2 and $N = 6$, type-3 and 4). Note that all these results are well obtained by choosing the control parameters: CR in the range [0.90, 1.00] and F in the range [0.25, 0.50].

All odd and even values of the switching angles have sets of patterns in both type-1 and type-2 (as shown in Figs. 3 and 4). However, there are only two switching patterns exist for $N = 2$ to 5. The pattern groups for $N = 2$ to 13 are shown in Table 1. Sets of patterns as mentioned in type-1 and/or type-2 are already reported in [1]-[10]. However, none of the papers [1]-[10] have investigated other potential set of solutions as well as shown in Figs. 5-6. Furthermore, four types of patterns for $N = 9$ have also been reported in [11] for all positive of M (the remaining four other types are for all negative of M). The still remaining question for the patterns in [11] is which one of the patterns gives a better performance compared to another.

In this paper, the multiple patterns performance is compared based on *THD* of the inverter output voltage (line-to-line voltage). An L - C filter is inserting between the inverter and a resistive load. Figure 7(a) presents a typical *THD* performance of type-1 and type-2 for $N = 3$ throughout all positive values of M ($0 \leq M \leq 1.15$). It shows that type-2 offers a better harmonic performance than type-1 and this has also been reported in [12], [13]. However,

there are no solutions found in [12], [13] when $M \geq 0.93$ (set-1 which corresponds to (ii) in Fig. 3) and $M \geq 0.91$ (set-2 which corresponds to (ii) in Fig. 4).

Table 1. Pattern Groups for $N = 2$ to 13

N	2,3,4,5	6,7,8,9	10,11,12,13
Type	1,2	1,2,3,4	1,2,3,4,5,6,7,8

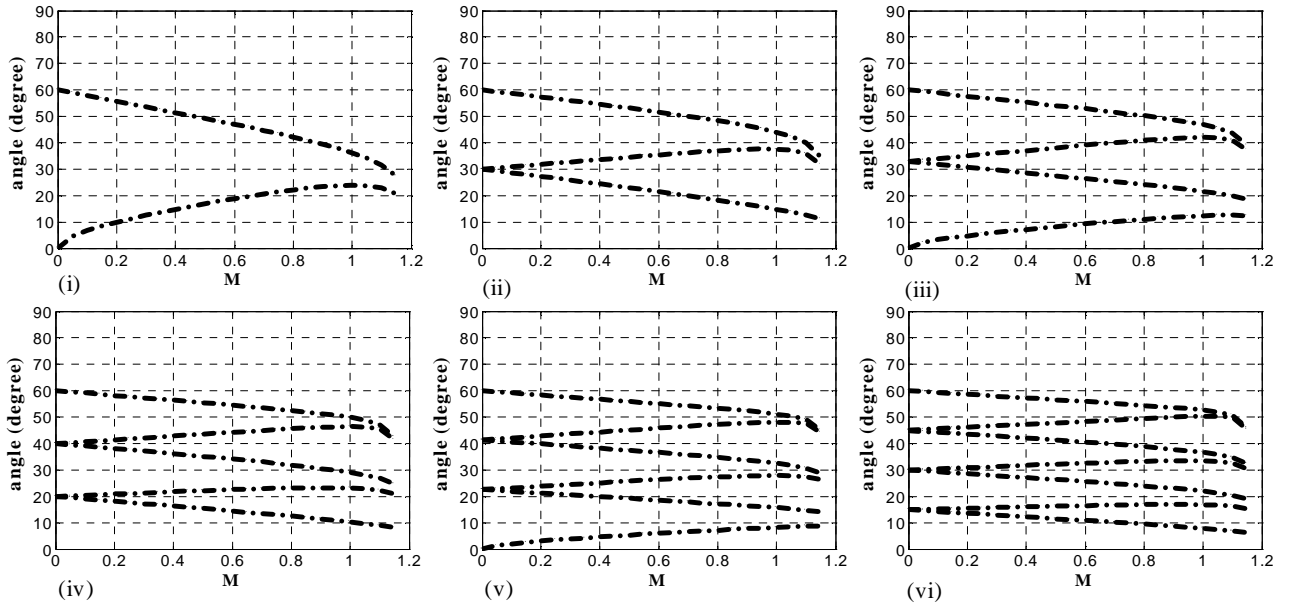


Figure3. Type-1 of switching patterns. (i) $N = 2$, (ii) $N = 3$, (iii) $N = 4$, (iv) $N = 5$, (v) $N = 6$, and (vi) $N = 7$

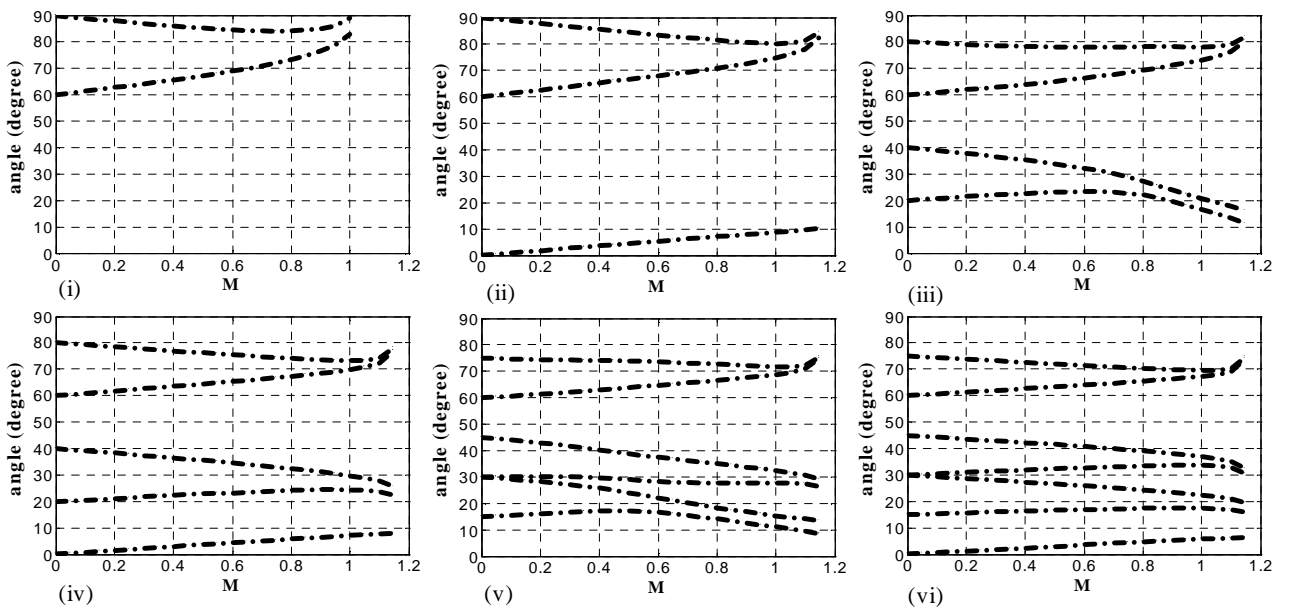


Figure4. Type-2 of switching patterns. (i) $N = 2$, (ii) $N = 3$, (iii) $N = 4$, (iv) $N = 5$, (v) $N = 6$, and (vi) $N = 7$

There are two types of patterns for $N = 2$ to 5 as presented in Figs. 3 and 4. Furthermore, there are two new types of patterns are found by employing $N = 6$ to 9 which are presented as type-3 and type-4 in Figs. 5 and 6. For all positive values of M , type-4 gives less *THD* than type-3 and the both types are better than type-2 and type-1 in their *THD* performances. Four other new types (type-5 to type- 8) which are obtained from $N = 10$ to 13 offer less *THD* compared to the previous types as shown in Fig. 7(b). Figure 7(b) shows a typical *THD* performance of type-1 to type-8 for all values of modulation indices ($0 \leq M \leq 1.15$).

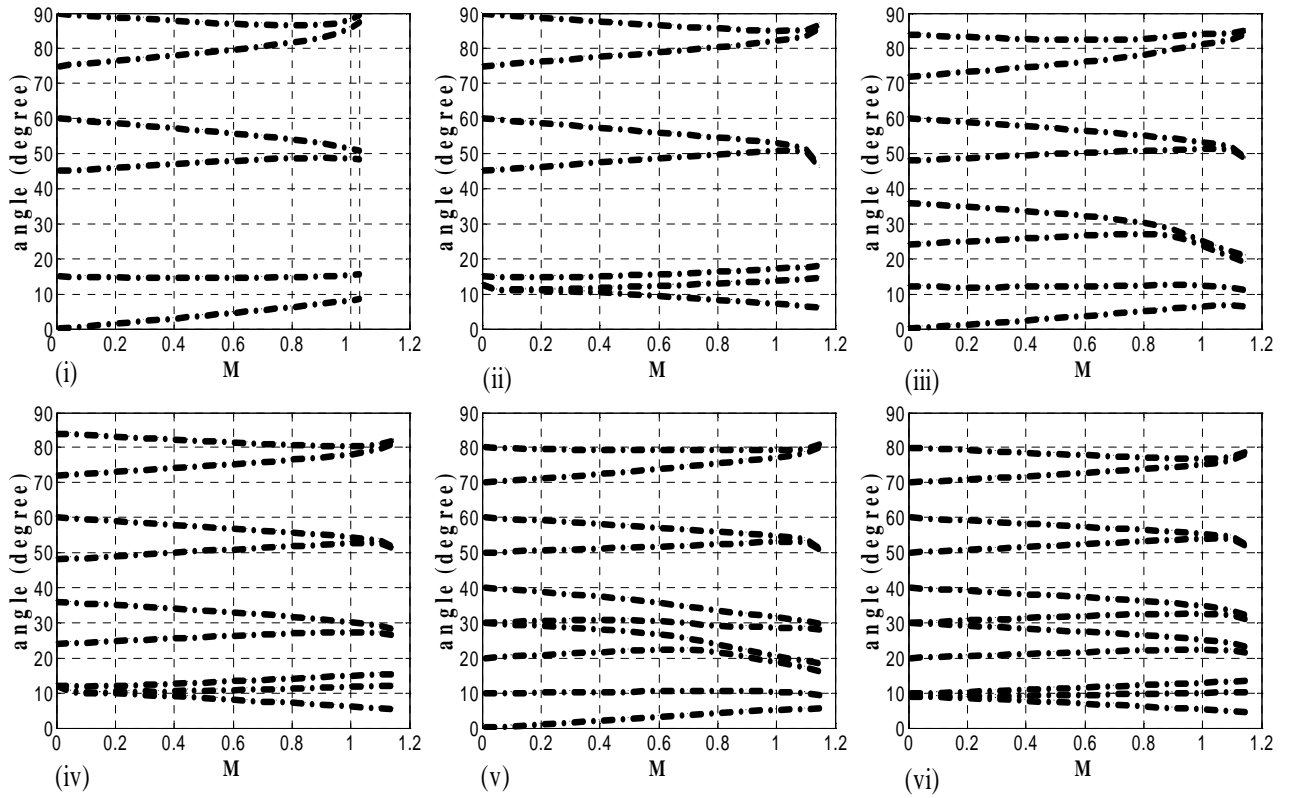


Figure5. Type-3 of switching patterns. (i) $N = 6$, (ii) $N = 7$, (iii) $N = 8$, (iv) $N = 9$, (v) $N = 10$, and (vi) $N = 11$

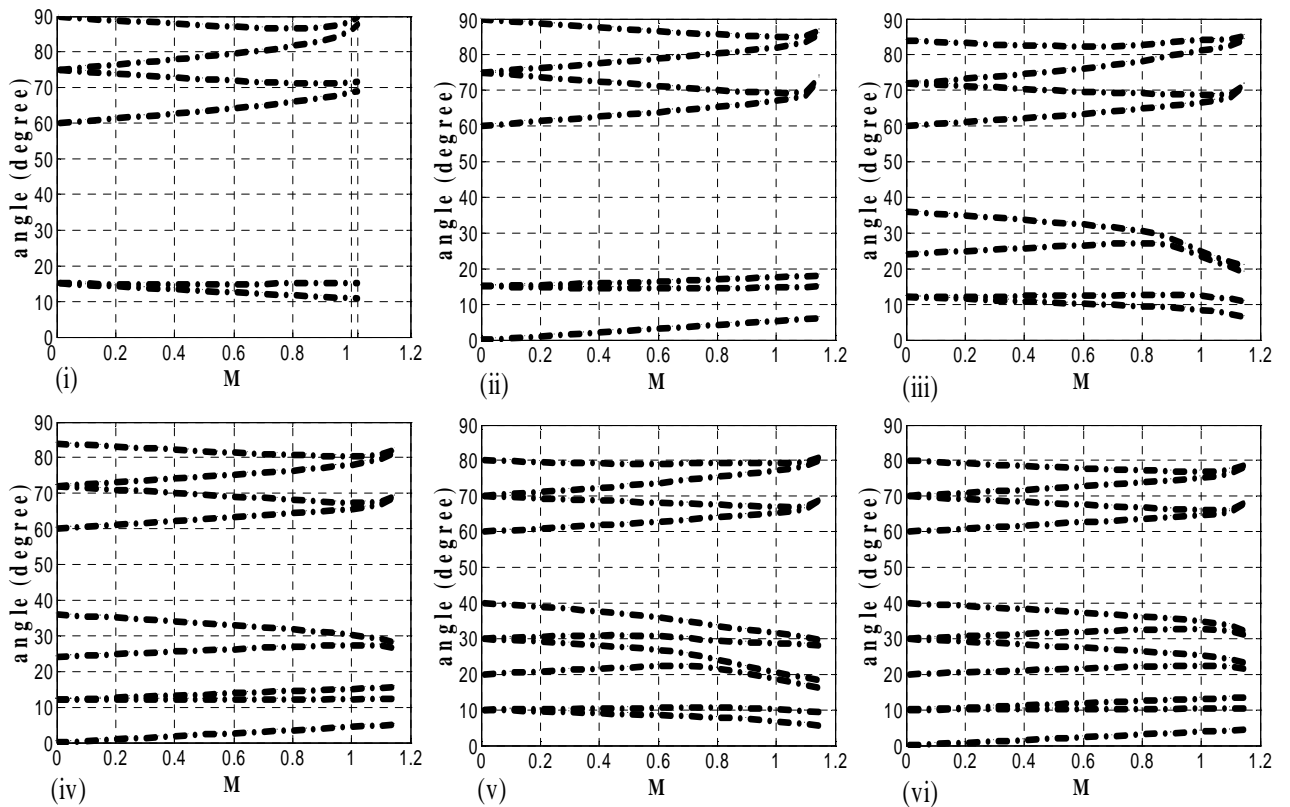


Figure6. Type-4 of switching patterns. (i) $N = 6$, (ii) $N = 7$, (iii) $N = 8$, (iv) $N = 9$, (v) $N = 10$, and (vi) $N = 11$

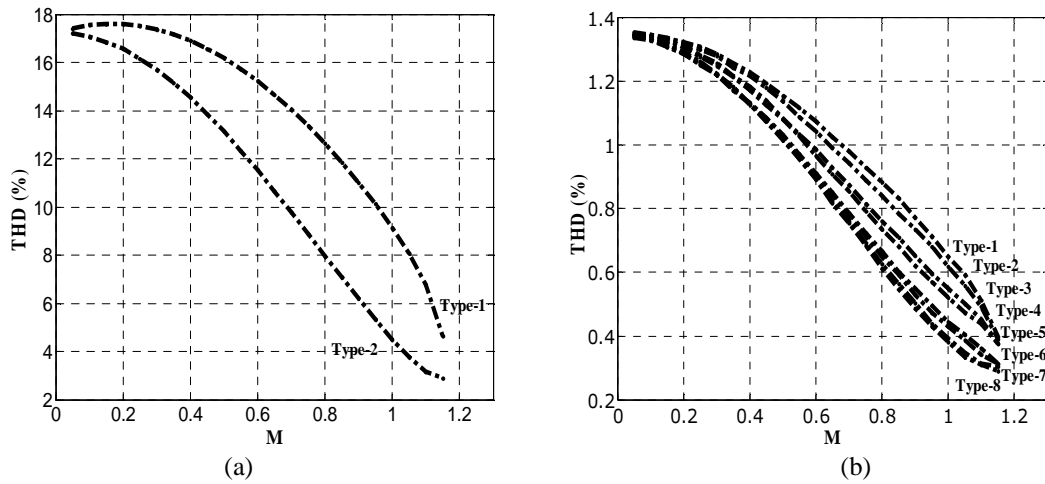


Figure 7. Total harmonic distortion as function of M : (a) for type-1 and type-2, (b) for type-1 to type-8

Figures 8 and 9 represent the various types of switching patterns available for $N = 12$ and $N = 13$, respectively. Figure 10 is a typical result obtained from the experiments for $N = 13$ and $M = 1$. Each type provides almost similar performance, but type-8 is clearly better than all others (see Table 2). Inspection these results also indicated that type-8 generates the lowest 41st (f_{41}) and 43rd (f_{43}) harmonics.

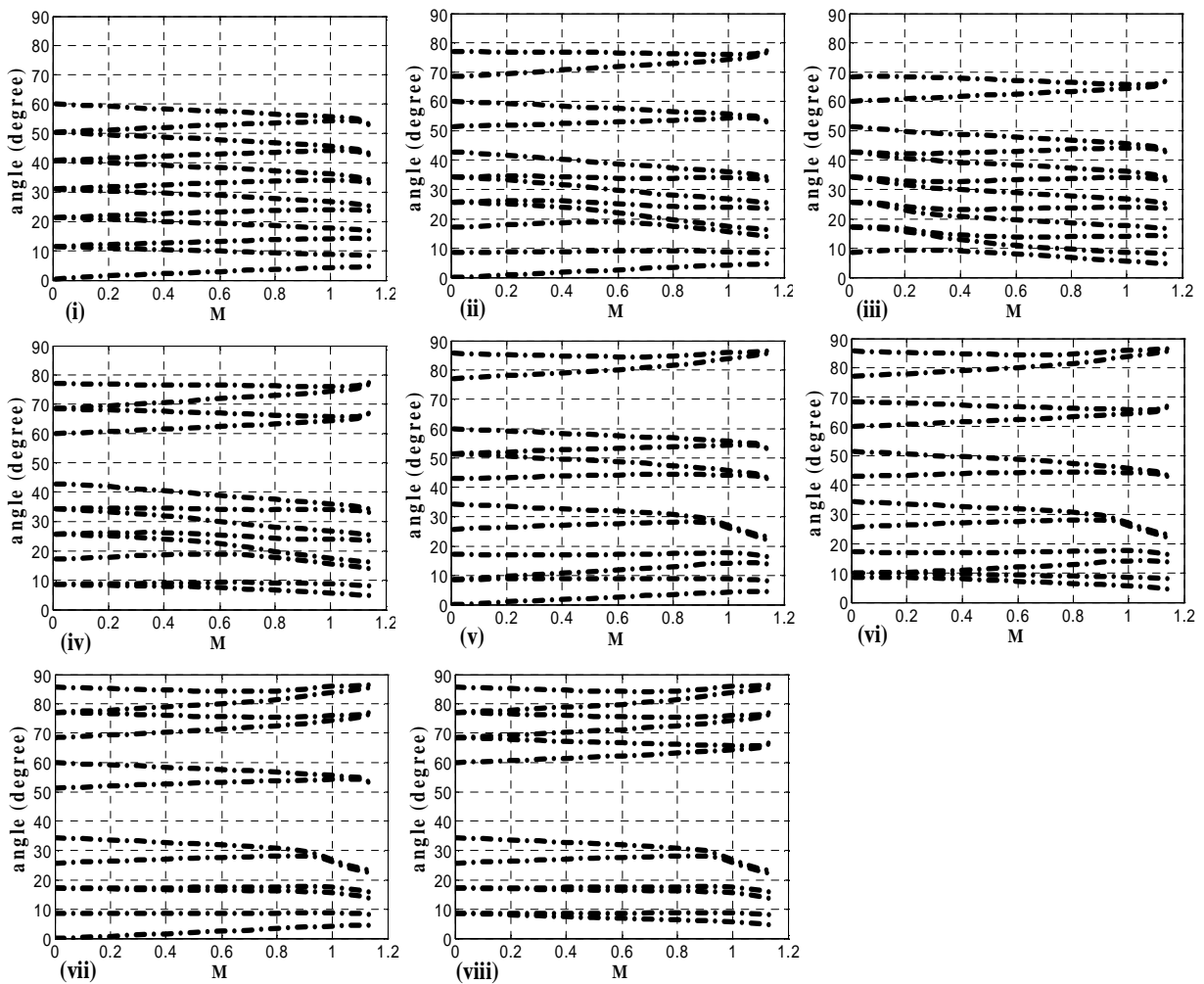


Figure 8. Switching patterns for $N = 12$. (i) type-1 to (viii) type-8

Table 2. Comparison THD of Various Patterns for $N = 13, M = 1$

	Type-1	Type-2	Type-3	Type-4	Type-5	Type-6	Type-7	Type-8
THD (%)	3.32	3.13	2.75	2.64	2.48	2.32	2.26	2.11
f_{41} (%)	2.98	2.88	2.6	2.52	2.15	2.09	1.95	1.89
f_{43} (%)	1.37	1.2	0.88	0.75	0.57	0.46	0.26	0.17

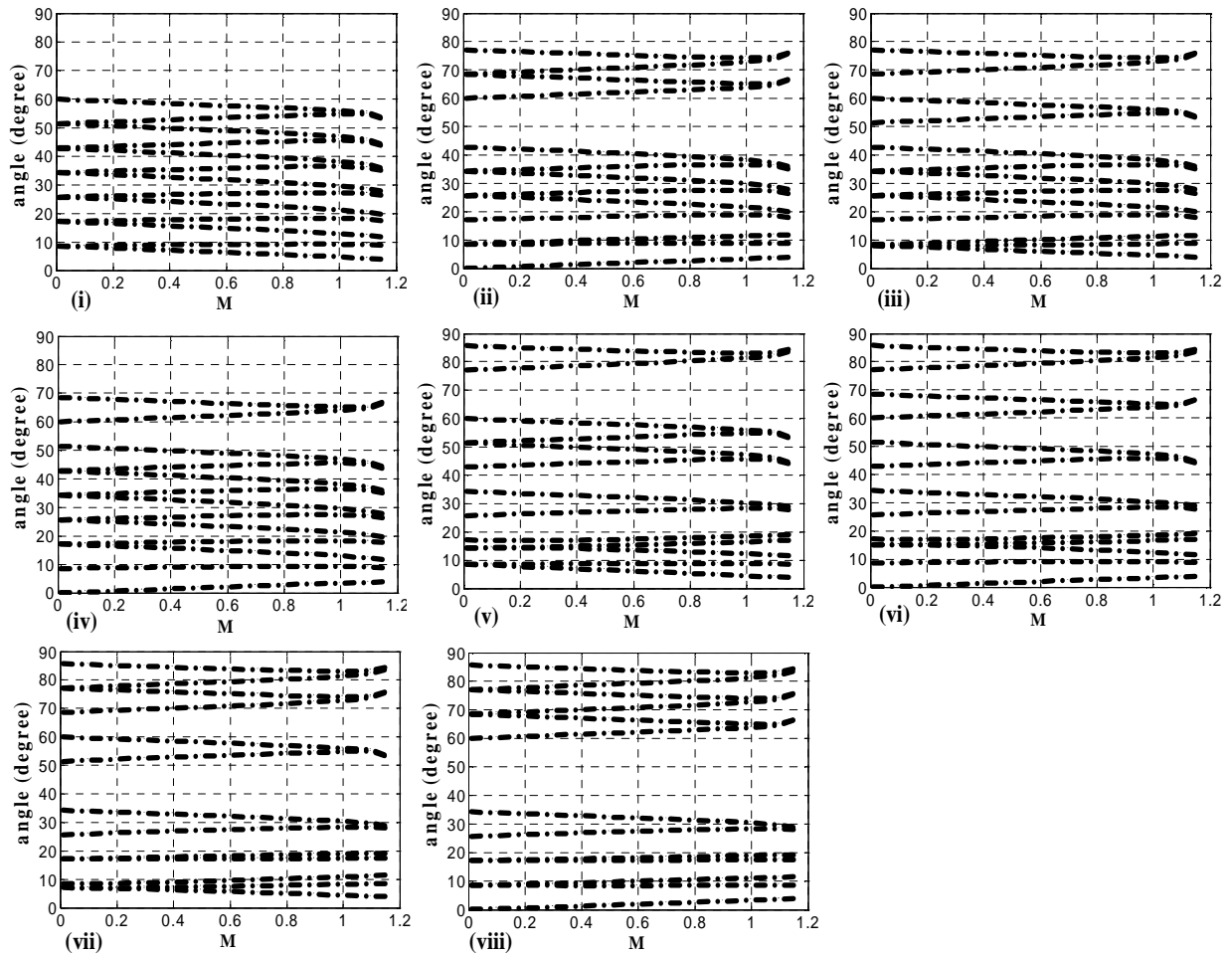


Figure 9. Switching patterns for $N = 13$. (i) type-1 to (viii) type-8

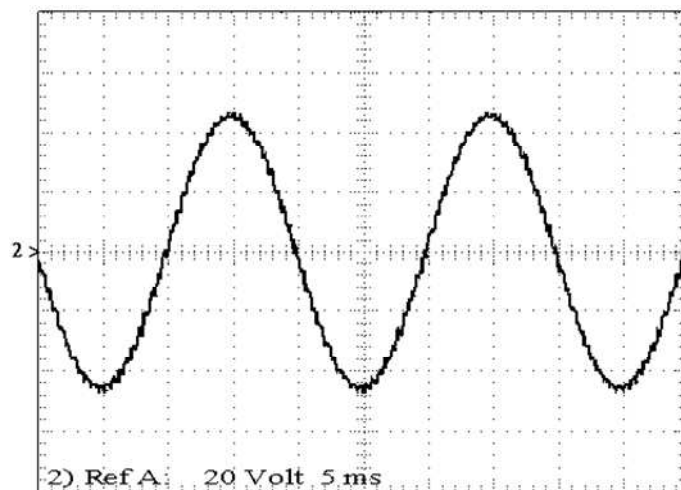


Figure10. Experimental result: the waveform of inverter output voltage for $N = 13$.

6. Conclusion

Optimum switching patterns for both odd and even values of angles in a three-phase SHEPWM inverter are investigated over the range $0 \leq M \leq 1.15$ using DE algorithms. The patterns are examined and classified based on the voltage output inverter harmonic performances. There are numerous patterns found for N switching angles that can be applied in the three phase SHWPWM inverter. It is confirmed that the different types of patterns offer varied performance when evaluated against the resulting THD. All switching patterns generate very low level THD after filtering, but one pattern offers the best THD of all.

References

- [1] J.A. Taufiq, B. Mellitt, and C.J. Goodman, "Novel algorithm for generating near optimal PWM waveforms for AC traction drives," in *IEE Proceedings B on Electric Power applications*, vol. 133, no. 2, pp. 85-94, Mar. 1986
- [2] P. Enjeti and J.F. Lindsay, "Solving nonlinear equation of harmonic elimination PWM in power control," *Electronics Letter*, vol. 23, no. 12, pp. 656-657, 1987
- [3] P.N. Enjeti, P.D. Ziogas, and J.F. Lindsay, "Programmed PWM technique to eliminate harmonics: A critical evaluation," *IEEE Transactions on Industrial Applications*, vol. 26, no. 2, pp. 302-316, Mar/Apr 1990.
- [4] J. Sun, S. Beineke, and H. Grotstollen, "DSP-based real-time harmonic elimination of PWM inverters," in *Proceedings 1994 IEEE Power Electronics Specialists Conference*, pp. 679-685
- [5] S.R. Bowes and P.R. Clark, "Regular-sampled harmonic-elimination PWM control of inverter drives," *IEEE Transactions on Power Electronics*, vol. 10, no. 5, pp. 521 – 531, 1995.
- [6] J. Sun, S. Beineke and H. Grotstollen, "Optimal PWM based on real-time solution of harmonic elimination equations," *IEEE Transactions on Power Electronics*, vol. 11, no. 4, pp. 612 – 621, 1996.
- [7] A. I. Maswood, S. Wei, and M.A. Rahman, "A flexible way to generate PWM-SHE switching patterns using genetic algorithm," in *Proceedings 2001 IEEE Applied Power Electronic Conference*, pp. 1130-1134.
- [8] F. Swift and A. Kamberis, "A new Walsh domain technique of harmonic elimination and voltage control in pulse width modulated inverters," *IEEE Transactions on Power Electronics*, vol. 8, no. 2, pp. 170-185, Apr 1993.
- [9] J.R. Espinoza, G. Jaos, J.I. Guzman, L.A. Moran, and R.P. Burgos, "Selective harmonic elimination and current/voltage control in current/voltage-source topologies: A unified approach," *IEEE Transactions on Industrial Electronics*, vol. 48, no. 1, pp. 71-81, Feb 2001.
- [10] J.N. Chiasson, L.M. Tolbert, K.J. McKenzie, and Z. Du, "A complete solution to the harmonic elimination problem," *IEEE Transactions on Power Electronics*, vol. 19, pp. 491-499, 2004.
- [11] T. Kato, "Sequential homotopy-based computation of multiple solutions for selected harmonic elimination in PWM inverters," *IEEE Transactions on Circuits and Systems-I: Fundamental, Theory and Applications*, vol. 46, no. 5, pp. 586 – 593, May 1999.
- [12] V.G. Agelidis, A. Balouktsis, and I. Balouktsis, "On Applying a minimization technique to the harmonic elimination PWM control: The bipolar waveform," *IEEE Power Electronics Letters*, vol. 2, no. 2, pp. 41 – 44, 2004.
- [13] V.G. Agelidis, A. Balouktsis, I. Balouktsis, and C. Cossar, "Multiple sets of solutions for harmonic elimination PWM bipolar waveform: Analysis and experimental verification," *IEEE Transactions on Power Electronics*, vol. 21, no. 12, pp. 415 – 421, Mar 2006.
- [14] V.G. Agelidis, A.I. Balouktsis, and C. Cossar, "On attaining the multiple solutions of selective harmonic elimination PWM three-level waveforms through function minimization," *IEEE Transactions on Industrial Electronics*, vol. 55, no. 3, pp. 996 – 1004, 2008.
- [15] R.A. Jabr, "Solution trajectories of the harmonic-elimination problem," in *IEE Proceedings Electric Power Applications*, vol. 153, no. 1, pp. 97 – 104, Jan 2006.
- [16] L.C. Woei, P.F. Yung, and H.P. Chun, "A simple approach to the realization of an FPGA-based harmonic elimination PWM generator," in *Proceedings of the 18th International Conference on Electrical Machines*, pp. 1-6, 2008
- [17] R. Storn, K.V. Price, "Differential evolution - a simple and efficient heuristic for global optimization over continuous spaces," *Journal of Global Optimization*, vol. 11, pp. 341-359, 1997

Bibliography of author



AyongHiendro was born in Ketapang, Indonesia. He received the B.Engdegree in electrical engineering from Tanjungpura University(UNTAN), Pontianak,Indonesia and the M.Eng. degreein electrical engineering from Bandung Institute of Technology (ITB), Bandung, Indonesia in 2000. He is currently a Senior Lecturer in the Department of Electrical Engineering, Faculty of Engineering, TanjungpuraUniversity.